Asymmetric Modulation and Blockade of the Delayed Rectifier in Squid Giant Axons by Divalent Cations

John R. Clay
Laboratory of Neurophysiology, National Institute of Neurological Disorders and Stroke, National Institutes of Health, Bethesda, Maryland 20892, and the Marine Biological Laboratory, Woods Hole, Massachusetts 02543 USA

ABSTRACT The effects of intracellular magnesium ions and extracellular calcium and magnesium ions on the delayed rectifier potassium ion channel, I_K, were investigated from intracellularly perfused squid giant axons. Ca_o^{+2} and Mg_o^{+2} both blocked I_K in a voltage-independent manner with a K_D of ~100 and 500 mM, respectively. This effect was obscured at potentials in the vicinity of the resting potential (~−60 mV) by a rightward shift of the steady-state I_K inactivation curve along the voltage axis. The addition of either calcium or magnesium ions to the extracellular solution also produced the well known shift of the I_K activation curve along the voltage axis. Ca_o^{+2} was approximately twice as effective in this regard as Mg_o^{+2}. The I_K activation kinetics were slowed by Ca_o^{+2}, but deactivation kinetics were not altered, as shown previously. Similar results were obtained with Mg_o^{+2}. The addition of magnesium ions to the intracellular perfusate shifted the activation curve along the voltage axis in the negative direction (without producing block) by approximately the same among as the Mg_o^{+2} shift of this curve in the positive direction. Moreover, Mg_i^{+2} substantially slowed the deactivation kinetics, whereas the effects of Mg_i^{+2} on activation kinetics at strongly depolarized potentials were relatively minor. At modest depolarizations, Mg_i^{+2} significantly reduced the delay before I_K activation. These results are essentially the mirror image of the effects on gating of extracellular divalent cations.

INTRODUCTION

The effects of extracellular divalent cations on voltage-gated ion channels are well known (Frankenhauser and Hodgkin, 1957; Gilly and Armstrong, 1982a,b; Armstrong and Cota, 1990). Specifically, the addition of these ions to the extracellular solution shifts the activation curve along the voltage axis in the depolarizing direction, and they also shift activation kinetics along the voltage axis more so than deactivation, or "tail" kinetics. The latter observation is inconsistent with simple surface charge theory. In contrast, surprisingly few results have been reported regarding the modulation of voltage-dependent gating by intracellular divalent cations, with the notable exception of Cukierman and Krueger (1991), who reported intracellular divalent cation effects on the batrachotoxin-modified sodium channel incorporated in planar lipid bilayers. Their work is complemented by the results in this study on the delayed rectifier current, I_K, from internally perfused squid giant axons with magnesium ions added to the internal perfusate. The main observation is that Mg_i^{2+} significantly alters the deactivation kinetics with relatively little effect on channel activation, except for a reduction in the delay that precedes activation produced by a relatively negative holding potential. In other words, the Cole and Moore (1960) effect is offset by Mg_i^{2+}. Other than this result, the effects of Mg_i^{2+} on activation and deactivation are in essence the mirror image of the effects of Ca_o^{2+} and Mg_o^{2+} on gating. Moreover, the effects of divalent cations on gating from either side of the membrane appear to be a discontinuous function of membrane potential. For example, an increase in Ca_o^{2+} slows activation kinetics even for relatively modest depolarizations ($V \sim -50$ mV), whereas tail current kinetics are unaffected for $V \sim -50$ mV. A serendipitous result from these experiments was the observation of a voltage-independent block of I_K by Ca_o^{2+} and Mg_o^{2+}, but not Mg_i^{2+}. This effect is obscured at holding potentials in the vicinity of the resting potential (~−60 mV) by a shift along the voltage axis of the steady state inactivation curve for I_K by Ca_o^{2+} and Mg_o^{2+} Some of these results have been reported in abstract form (Clay, 1993).

MATERIALS AND METHODS

Experiments were performed on voltage-clamped, internally perfused squid giant axons at the Marine Biological Laboratory (Woods Hole, MA) primarily in May and early June using techniques described in Clay and Shlesinger (1983). The temperature of the experimental chamber ranged between 7 and 14°C. In any single experiment the temperature was maintained constant to within 0.1°C by a negative feedback circuit connected to a Peltier device. The sodium ion current was blocked by tetrodotoxin (TTX; Sigma Chemical Co., St. Louis, MO). The intracellular solution for the experiments in which the extracellular divalent cation concentration was modified consisted of 250 K glutamate, 50 KF, and 400 sucrose (pH = 7.2; all solutions given in mM). The extracellular solutions in these experiments consisted of 1, 5, 10, 20, 50, or 100 $CaCl_2$ with 460, 450, 445, 430, 360, or 310 NaCl, respectively, and 10 Tris-HCl (pH = 7.2) and 1 μM TTX, (referred to below as 1, 5, 10, 20, 50, or 100 Ca_o^{2+}); or 1, 100, or 200 $MgCl_2$ with 460, 310, or 160 NaCl, respectively, and 10 Tris-HCl and 1 μM TTX (referred to below as 1, 100, or 200 Mg_o^{2+}). The tail currents illustrated in Fig. 5 *C* were obtained with 100 KCl and an equal reduction of the NaCl concentration. Similarly, the inactivation curves for I_K in Fig. 4 were obtained with 150 KCl and an equal reduction of NaCl. The extracellular solution for the experiments with intracellular magnesium ions

Received for publication 7 November 1994 and in final form 28 July 1995.
Address reprint requests to J. R. Clay, National Institutes of Health, Building 36; Room 2C02, Bethesda, MD 20892. Tel.: 301-496-7711; Fax: 301-402-1565; E-mail: jrclay@nih.gov.

0006-3495/95/11/1773/00 $2.00

consisted of 10 $CaCl_2$, 50 $MgCl_2$, 440 NaCl, 10 Tris-HCl, and 1 μM TTX. The tail currents shown in Fig. 5 *F* were obtained in the same solution but with 50 mM NaCl replaced by 50 mM KCl. The intracellular solution in these experiments consisted of 300 K glutamate and 400 sucrose in control conditions (0 Mg_i^{2+}), or 300 sucrose, 300 K glutamate and 100 $MgCl_2$ (100 Mg_i^{2+}). The osmolarity of both control and test solutions was in the 1000–1200 mOsm range. Liquid junction potentials were <3 mV. The results in this report have not been corrected for these relatively small offsets.

RESULTS

Blockade of I_K by Ca_o^{2+} and Mg_o^{2+}

The effects of Ca_o^{2+} and Mg_o^{2+} on I_K are illustrated in Fig. 1, (*A* and *B*) and (*C* and *D*), respectively (different preparation in each case). A relatively negative holding potential (−90 mV) was used here and throughout most of the experiments in this study to eliminate any effects of I_K inactivation, as noted below. The step potentials for each panel in Fig. 1 were −30, −20, ··· +10 mV. A clear blockade of I_K was apparent with Ca_o^{2+}, and, to a lesser extent, with Mg_o^{2+}. This effect was reversible, as illustrated by the records above Fig. 1 *A* in which the current trace elicited by a step to +20 mV is shown from another axon with either 20 or 100 Ca_o^{2+} (Fig. 1, *results superimposed*) and then after a return of the external solution to 20 Ca_o^{2+}. The blockade was voltage-independent as illustrated below (Fig. 2). The degree of blockade was determined, quantitatively, from the reduction of maximum outward current elicited by a step to +20 mV, for which maximal channel activation occurred for $Ca_o^{2+} \leq 100$ mM. The degree of block as a function of calcium ion concentration is shown in the inset above Fig. 1 *B* (different preparation from that shown in Fig. 1, *A* and *B*). The curve is a best fit of these results by the expression $(1 + Ca_o^{2+}/K_D)^{-1}$, where K_D is the dissociation constant of binding of a calcium ion to a blocking site somewhere on or near the channel, with K_D = 33 mM. The pooled result for this parameter was K_D = 90 ± 59 mM (±SD; n = 7). The corresponding result for blockade by Mg_o^{2+} was K_D = 497 ± 147 mM (n = 4). A similar effect was not observed with Mg_i^{2+}, as indicated by the results in Fig. 1, *E* and *F*.

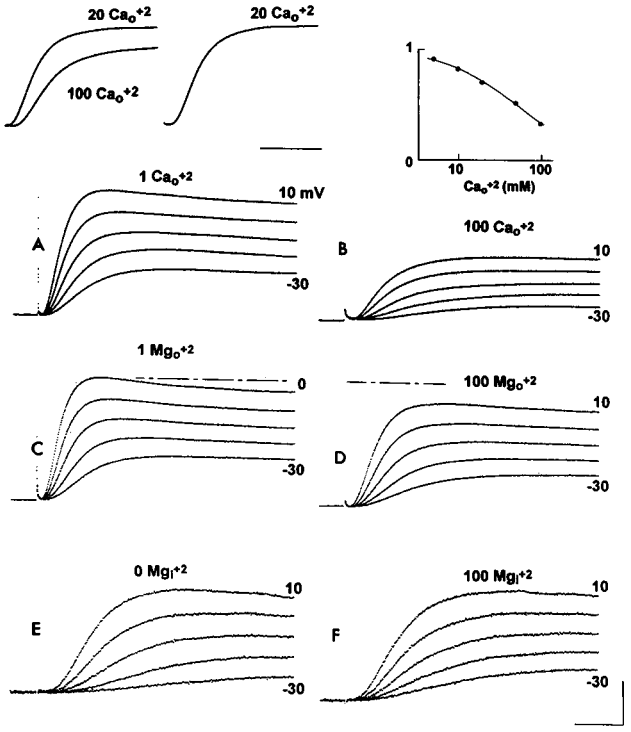

FIGURE 1 Effects of Ca_o^{2+} (*A* and *B*); Mg_o^{2+} (*C* and *D*); and Mg_i^{2+} (*E* and *F*) on I_K. Step potentials in each case were −30, −20, ··· +10 mV. Duration of the steps was 20 ms. Divalent cation conditions as shown (see Materials and Methods). Holding potential for all results was −90 mV. All records leak corrected. T = 14°C for *A–D*, 8°C for *E* and *F*. Horizontal calibration is 5 ms; vertical calibration is 1 mA·cm^{-2} for *A–D*; 0.5 mA·cm^{-2} for *E* and *F*. The inset above *B* illustrates the blockade of I_K (determined as described in the text) from another preparation as a function of Ca_o^{2+}. The records above *A* illustrate reversibility of Ca_o^{2+} blockade with 20 and 100 Ca_o^{2+}. The two results superimposed on the left were elicited by a voltage step to +20 mV in 20 and then 100 Ca_o^{2+}. The result to the right of these records illustrates the current elicited after a return to 20 Ca_o^{2+}.

The voltage-independence of I_K blockade by Ca_o^{2+} is illustrated in Fig. 2 for 20 and 100 Ca_o^{2+}. The membrane potential was stepped in either condition to +30 mV for 12 ms followed by steps to the potentials indicated. The degree of reduction of I_K in 100 relative to 20 Ca_o^{2+} was 0.76–78 regardless of membrane potential, as shown by the plot below the records in Fig. 2, which contains results from three different preparations.

Effect of Ca_o^{2+} on I_K inactivation

The delayed rectifier has an inactivation process with very slow kinetics having at least two time constants, 1 and 30 s,

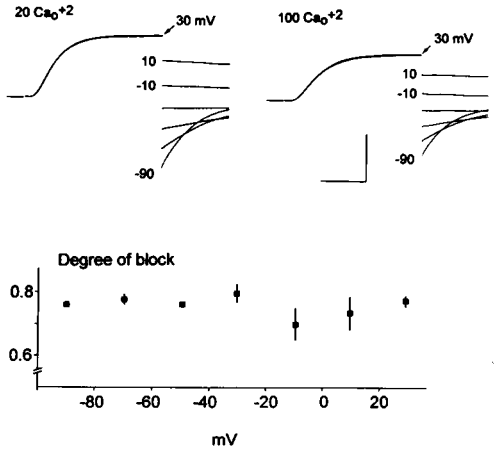

FIGURE 2 Voltage-independence of Ca_o^{2+} blockade. The membrane potential was stepped to +30 mV for 12 ms in either 20 or 100 Ca_o^{2+}, followed by a second step to +10, −10, ··· −90 mV with a 2-s rest interval between each of these two pulse sequences. Horizontal calibration is 4 ms, vertical calibration is 2 mA·cm^{-2}. The results below the records illustrate the reduction in current in 100 Ca_o^{2+} relative to 20 Ca_o^{2+} either at the end of the prepulse (+30 mV) or 100 μs following the second step (10, −10, ··· −90 mV) for three different preparations (mean ± SD). Holding potential = −90 mV; K_o = 100 mM.

respectively (Ehrenstein and Gilbert, 1966; Chabala, 1984; Clay, 1989). Moreover, this process plays a role in determining the fraction of conductance available for activation during the action potential under physiological conditions. In particular, ~20% of I_K is inactivated at the resting potential (~ −60 mV) in filtered seawater (Clay, 1989). The inactivation effect can be most readily observed in steady state conditions by using various different holding potentials in the −100 to −50 mV range (Clay, 1989, 1990). For example, the results in Fig. 3, *A* and *C* were obtained in 20 Ca_o^{2+} with a holding potential of either −90 or −60 mV (Fig. 3, *A* and *C*, respectively). The term holding potential in this case implies a steady state condition. That is, the membrane potential was held at either level for 5 min before steps were made to the potentials indicated (−40, −30, ··· 0 mV). The results in Fig. 3, *A* and *C*, indicate a clear reduction in the amount of available I_K at −60 mV, which is attributable to the inactivation process. The results in Fig. 3 *B* with 100 Ca_o^{2+} (holding potential = −90 mV) illustrate the block of I_K by calcium ions noted above. Very little change was apparent in these results after a change of holding potential to −60 mV (Fig. 3 *D*), because of a rightward shift along the voltage axis of the steady state inactivation curve (Fig. 4). That is, the I_K amplitudes elicited by the steps to −10 and 0 mV in Fig. 3, *C* and *D*, actually indicate an increase in I_K with a holding potential of −60 mV following a change of Ca_o^{2+} from 20 to 100 mM. The explanation for this paradoxical result is that the increase in Ca_o^{2+} effectively removes steady state inactivation at −60 mV, thereby more than compensating for the reduction in I_K produced by Ca_o^{2+} blockade.

Further results concerning the effect of Ca_o^{2+} on inactivation are shown in Fig. 4. The steady state inactivation curve was measured in these experiments following the procedure previously used to determine the effects of pH_i on this parameter (Clay, 1990). Specifically, the membrane potential was held at the level indicated on the abscissa of Fig. 4 for at least 5 min. It was then stepped for 15 ms to −20 mV, which was close to the potassium ion equilibrium potential for the conditions of these results (300 K_i/150 K_o). This prepulse activated the conductance without producing

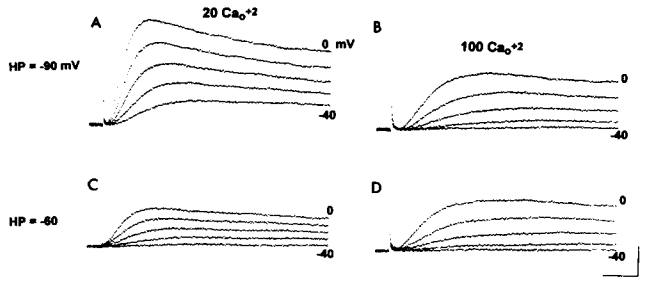

FIGURE 3 Effect of holding potential on I_K results with different levels of Ca_o^{2+}. Holding potential for *A* and *B* was −90 mV, and −60 mV for *C* and *D*. Ca_o^{2+} for *A* and *C* was 20 mM, and 100 mM for *B* and *D*. Records leak current corrected. Horizontal calibration was 5 ms; vertical calibration was 1 mA·cm^{-2}. Step potentials as indicated.

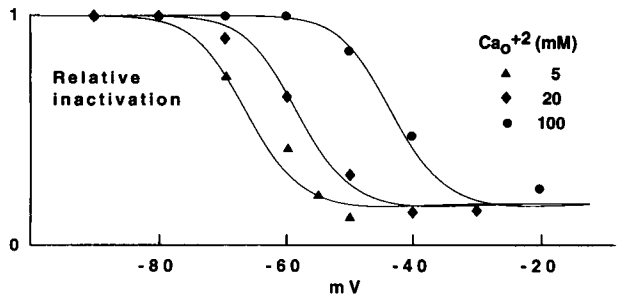

FIGURE 4 Steady-state inactivation of I_K as a function of Ca_o^{2+}. K_o = 150 mM. Ca_o^{2+} as indicated. Results obtained as described in the text and in Clay (1990). The results for 20 and 100 Ca_o^{2+} were taken from a single preparation. The results for 5 Ca_o^{2+} represent the average of two other preparations. The curves represent the probability, p_{nb}, that the I_K channel is not inactivated in the steady-state in the three state model of inactivation given in Clay (1989) with $p_{nb} = (1 + a/b + ac/(bd) + ace/(bdf))^{-1}$, where $a = (1 + \exp(-(V + V_o + 50)/5))^{-1}$; $b = 1.75(1 + \exp(-(V + V_o + 65/10))$; $c = 1 + \exp(-(V + V_o + 57)/10)$; $d = 2(1 + \exp(-(V + V_o + 50)/15))$; $e = 0.2(1 + \exp(-(V + V_o + 35)/8))$; and $f = 0.015(1 + \exp(-(V + V_o + 40)/5))$, all parameters in s^{-1} and all voltages in mV, with V_o = 13, 5, and −9 mV for Ca_o^{2+} = 5, 20, and 100 mM, respectively.

significant net current. The instantaneous current-voltage relation was then determined with steps to +20, 0, −40, and −60 mV. The averaged reduction of current elicited from each test step was used as a measure of steady state inactivation, as indicated by the symbols in Fig. 4. All results were normalized relative to currents obtained with a holding potential (HP) of −90 mV, which was used for each level of Ca_o^{2+} in these experiments. (The theoretical descriptions of the results in Fig. 4 were taken from the model of inactivation described in Clay (1989).) These results complement and extend those illustrated in Fig. 3. For example, the significant, relative reduction of I_K amplitude with *HP* = −60 relative to *HP* = −90 mV with 20 Ca_o^{2+} is consistent with Fig. 3, *A* and *C*, whereas the relative lack of inactivation at −60 relative to −90 mV for 100 Ca_o^{2+} is consistent with Fig. 3, *B* and *D*.

Effects of Ca_o^{2+}, Mg_o^{2+}, and Mg_i^{2+} on gating

A summary of the effects of the divalent cations used in this study on I_K kinetics is illustrated in Fig. 5. A change in Mg_o^{2+} from 1 to 100 mM produced a marked slowing of activation at +10 mV (Fig. 5 *A*) similar to the effects of Ca_o^{2+} (Armstrong and Matteson, 1986). No effect of Mg_o^{2+} or Ca_o^{2+} on tail current kinetics was observed, as illustrated in Fig. 5 *C* for Ca_o^{2+} with 100 K_o and a test potential of −110 mV. A significant block of tail current by Ca_o^{2+} was observed, similar to the results given above, but the time constant of the deactivation kinetics was not altered. In contrast, the addition of 100 mM $MgCl_2$ to the intracellular perfusate produced a relatively minor effect on activation at strong depolarizations (Fig. 5 *B*; voltage step to +20 mV). A slight decrease of the delay before onset of the current was observed as indicated by the arrows in Fig. 5 *B*, but the

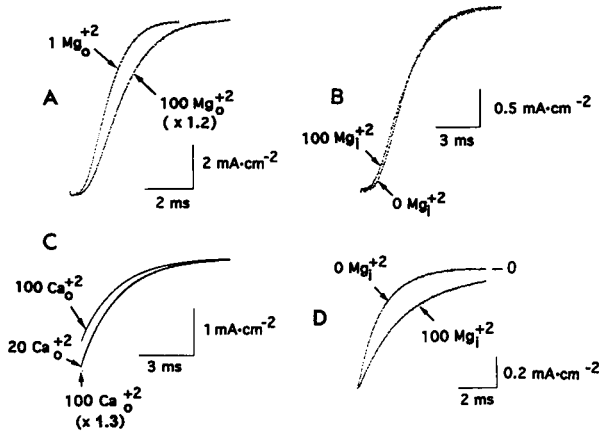

FIGURE 5 Effects of Mg_o^{2+}, Ca_o^{2+}, and Mg_i^{2+} on I_K kinetics. (*A*) Voltage steps to +10 mV in either 1 or 100 Mg_o^{2+}. The 100 Mg_o^{2+} result has been scaled by a factor of 1.2. (*B*) Voltage steps to +20 mV with either 0 or 100 Mg_i^{2+}. (*C*) Effect of Ca_o^{2+} on tail current at −110 mV after a 10 ms prepulse to −20 mV, K_o = 100, with Ca_o^{2+} equal to either 20 or 100 mM. The 100 Ca_o^{2+} result is also shown scaled by a factor of 1.3. (*D*) Tail currents in either 0 or 100 Mg_i^{2+} at −90 mV. Calibrations are as indicated.

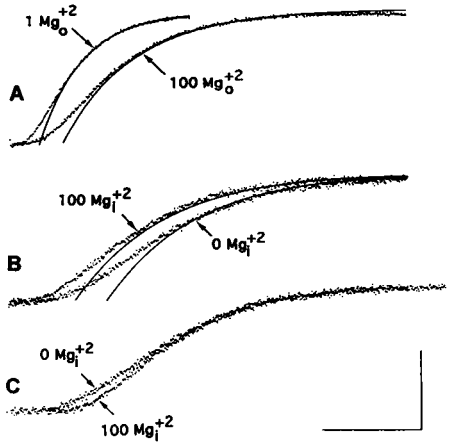

FIGURE 6 (*A*) Effect of a change in Mg_o^{2+} on activation kinetics with a voltage step to −20 mV. Holding potential = −90 mV. The theoretical curves are fits to the latter phase of activation of each result with a time constant of 1.95 and 3.5 ms for the 1 and 100 Mg_o^{2+} results, respectively. (*B*) Effect of 100 Mg_i^{2+} on I_K activation with a voltage step to −20 mV. Holding potential = −90 mV. The time constants of the exponential curves are 4.3 and 4.4 ms, for the 0 and 100 Mg_i^{2+} result, respectively. (*C*) Same results as in *B* with the 100 Mg_i^{2+} record shifted 2 ms rightward along the time axis. Calibrations are 5 ms for *A–C* and 1 mA·cm^{-2} for *A* and 0.5 mA·cm^{-2} for *B* and *C*.

time constant of activation after the delay was unaltered. In contrast, a marked slowing of deactivation kinetics was observed at hyperpolarized potentials (Fig. 5 *D*; −90 mV). The pooled result for the relative increase of the tail current time constant at −90 mV was 190 ± 41% (n = 4). A significant concern with the result in Fig. 5 *D* is the possibility that it might be due to an increase of ionic strength in these experiments (see Materials and Methods). A control result that argues against this possibility is the lack of effect on the tail current time constant after the addition of 300 mM CsF to the intracellular perfusate (Clay, 1985; Fig. 3B). Moreover, in previous experiments K_i was raised from 300 to 500 mM without altering the activation curve (Clay, 1991; result not shown). Consequently, the results reported here with 100 Mg_i^{2+} are attributable to divalent cation effects rather than to changes of ionic strength of the intracellular perfusate.

An additional effect of Mg_i^{2+} on activation gating is illustrated in Fig. 6, *B* and *C*, for modest depolarizations. Specifically, 100 Mg_i^{2+} significantly reduced the delay preceding activation of the conductance with a step to −20 mV (HP = −90 mV) without altering the time constant of the latter part activation (Fig. 6 *B*). (This effect is also discernible in the records for the +20 mV steps in Fig. 5 *B*.) Indeed, the records in Fig. 6 *B* largely superpose after translation along the time axis, as shown in Fig. 6 *C*, in a manner reminiscent of the Cole and Moore (1960) effect. That is, the delay preceding activation of I_K with a depolarizing step is significantly increased by a relatively negative prepulse, or holding level, as is the case with the control result in Fig. 6 *B* for which HP = −90 mV, and this delay was reduced by 100 Mg_i^{2+} although the control and test results do not completely superpose after time translation, as is true also for the Cole and Moore (1960) effect (Clay and Shlesinger, 1982). For comparison, the effect of Mg_o^{2+} with a step to −20 mV is shown in Fig. 6 *A*. The slowing of activation produced by 100 Mg_o^{2+} is not well characterized by a shift of the records along the time axis. Rather, the latter phase of activation is significantly slowed, as indicated by the description of this part of the records by the single exponential curves shown in Fig. 6 *A*. (A similar analysis is shown in Fig. 6 *B*.)

Effects of Ca_o^{2+}, Mg_o^{2+}, and Mg_i^{2+} on channel activation

The results in Figs. 5 and 6 are further amplified by the analysis in Fig. 7 *A* and B, in which representative activation curves for 10 and 100 Ca_o^{2+} and 0 and 100 Mg_i^{2+} are shown, respectively. These results were obtained after the procedure illustrated in part by the upper inset of Fig. 7, which contains records elicited by steps to −50 and −30 mV with 1 mM Ca_o^{2+}. The currents used to obtain the activation curve are illustrated by the arrows to the right of each record labeled I_o. This current is a product of the relative steady state activation, which, is given by n_∞^4 (V) in the Hodgkin and Huxley (1952) model of I_K, and the fully activated current voltage relation. The latter quantity is a nonlinear function of driving force, ($V - E_K$), with a voltage-dependence that is well described, phenomenologically, by the Goldman, Hodgkin, and Katz (GHK) relation (Goldman, 1943; Hodgkin and Katz, 1949; Clay and Shlesinger, 1983; Clay, 1991). That is, $I_K \sim (qV/kT) \cdot (\exp(q(V - E_K)/kT) - 1)/(\exp(qV/kT) - 1)$, where q, k, and T have their usual meanings, with $kT/q \sim 24$ mV at 10°C. For the conditions of these experiments, i.e., K_o = 0, the voltage-dependence of this expression reduces to

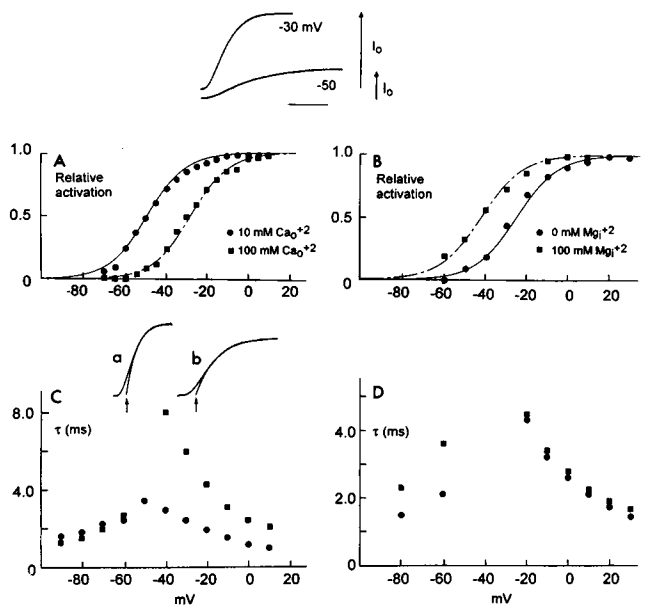

FIGURE 7 (*A* and *B*) Voltage shift produced by changing Ca_o^{2+} from 10 to 100 mM (*A*) or Mg_i^{2+} from 0 to 100 mM with 10 Ca_o^{2+} and 50 Mg_o^{2+} in the external solution (*B*). Experimental results obtained from the steady-state current (illustrated by the records above *A* for 1 Ca_o^{2+}; horizontal calibration 5 ms) following the procedure described in the text. The theoretical curves correspond to (*A*) $(1 + \exp(-zq(V - V_{1/2})/kT)^{-1}$, where $z = 2.7$ and $V_{1/2} = -49$ and -28 mV for 10 and 100 Ca_o^{2+}, respectively, and (*B*) $z = 2.5$ and $V_{1/2} = -25$ and -42 mV for 0 and 100 Mg_i^{2+}, respectively. (*C* and *D*) Effects of a change in divalent cations on kinetics for the corresponding conditions in *A* and *B*, respectively. The tail current time constants ($V < -50$ mV) were obtained from best fits of a single exponential to the corresponding experimental records. The activation results ($V > -50$ mV) were obtained from a fit to the final rising phase of activation currents, as indicated by *a* and *b* above *C*, which correspond to $V = 0$ for 10 and 100 Ca_o^{2+}, respectively. (The time constant at $V = -50$ mV with 100 Ca_o^{2+} (not shown), which was obtained from activation kinetics, was 12.3 ms.) The results in *D* were obtained as in Fig. 6 *C*.

$f_o(V) = (V/24)(\exp(V/24)/(\exp(V/24) - 1)$, which was used to obtain the results in Fig. 7, *A* and *B*. That is, I_o at each potential indicated on the abscissa of Fig. 7 was divided by f_o. The results of this procedure describe a curve that reached a saturating value at $V \sim 0$ mV, depending upon the divalent cation conditions. For example, the curve saturated at $V \sim -10$ mV for $Ca_o^{2+} = 10$ mM, as indicated in Fig. 7 *A*. This saturating value was used to normalize the corresponding results for all potentials. Examples of the final results of this procedure are shown in Fig. 7, *A* and *B*. An increase in Ca_o^{2+} produced the well known rightward shift of the activation curve along the voltage axis (Fig. 7 *A*), and the addition of magnesium ions to the intracellular perfusate produced a leftward shift of the curve along the voltage axis (Fig. 7 *B*), as shown also by Perozo and Bezanilla (1990) in dialyzed axons. The theoretical curves in Fig. 7, *A* and *B*, correspond to the Boltzmann relation, as described in the legend of Fig. 7. Pooled results for the midpoints of the activation curve for some of the conditions used in this study are -55 ± 2.5 mV ($\pm$ SD; $n = 3$) for 1 Ca_o^{2+}; -32 ± 6 mV ($n = 5$) for 100 Ca_o^{2+}; -58 and -52 mV ($n = 2$) for 1 Mg_o^{2+}; and -41 ± 4 mV ($n = 3$) for 100 Mg_o^{2+}. That is, a change in Ca_o^{2+} from 1 to 100 mV produced a 23 ± 6.5 mV depolarizing shift of the activation curve, whereas a change in Mg_o^{2+} from 1 to 100 mM produced a 14 mV shift. Finally, the addition of 100 mM $MgCl_2$ to the intracellular perfusate shifted the curve 17 ± 5 mV ($n = 4$) in the hyperpolarizing direction.

Initial conditioning of the effect of divalent cations on gating?

The effects of divalent cations on gating kinetics are further illustrated in Fig. 7, *C* and *D*. The time constant of channel deactivation ("tail" currents) for the various conditions illustrated were obtained from a best fit to these results of a single exponential. The activation time constants were obtained from a single exponential fit to the records starting from the 50% point of maximum current amplitude, as illustrated by records *a* and *b* shown above Fig. 7 *C*. This procedure essentially gives the time constant of the final, slow phase of channel activation. (A similar analysis is shown in Fig. 6, *A* and *B*.) These results are illustrated in Fig. 7, *C* and *D* ($V \geq -50$ mV) for the conditions of the experiments given in Fig. 7, *A* and *B*, respectively. The procedure is admittedly ad hoc, but it does illustrate the differential effects of extra- and intracellular divalent cations on activation kinetics. In particular, the time constant of the slow phase of activation is significantly increased by an increase in extracellular divalent concentration, whereas it is altered very little by the addition of divalent cations to the intracellular solution, as shown in Fig. 6 *B*. One striking aspect of these results (especially evident in Fig. 7 *C*) is an apparent discontinuity with membrane potential of the effect of a change in divalent cation concentration on gating. At strongly depolarized potentials the time constant for gating is determined almost exclusively by the activation parameter. Similarly, at strongly hyperpolarized potentials gating is determined almost exclusively by the deactivation parameter. The differential effects of divalent cations on these two processes originally reported by Gilly and Armstrong (1982a,b) can be readily accounted for by a differential effect of divalent cations on activation and deactivation, respectively, as suggested by Gilly and Armstrong (1982a,b). However, the situation in the vicinity of the resting membrane potential ($V \sim -60$ to -50 mV) is less clear. In this range of membrane potentials the macroscopic time constant is determined almost equally by the activation and deactivation parameters. If a change in divalent cation concentration preferentially affects only activation, the macroscopic time constant should, nevertheless, be a continuous function of membrane potential. The results in Fig. 7 *C* and in previous reports (cf. Spires and Begenisich, 1992) suggest otherwise. This point is further illustrated by the results in Fig. 8 in which activation kinetics in 20 and 100 Ca_o^{2+} were measured with a voltage step to -45 mV from a holding potential of -90 mV, and deactivation

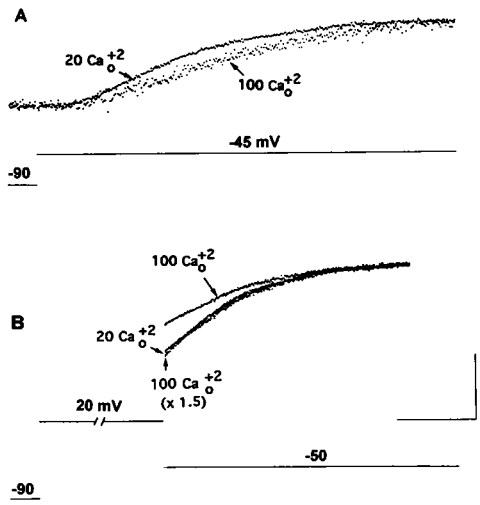

FIGURE 8 Results that suggest an initial conditioning of the potassium channel-calcium ion interaction by membrane potential. (*A*) Records elicited by a voltage step to −45 mV from a holding potential of −90 mV in either 20 or 100 Ca_o^{2+} with the latter scaled upward by a factor of 3.4. (*B*) Tail currents at −50 mV after a voltage prepulse to 20 mV for 15 ms. The current level at the end of these records was set to 0, and the 100 Ca_o^{2+} result is also shown scaled upward by a factor of 1.5. Same preparation as in (*A*) Horizontal calibration, 5 ms; vertical calibration 0.2 $mA \cdot cm^{-2}$. The time constant of these results was 5.75 and 5.9 ms for 20 and 100 Ca_o^{2+}, respectively.

kinetics at −50 mV were measured after a prepulse to +20 mV. The results in Fig. 8 *A* once again illustrate a significant slowing of activation after an increase of Ca_o^{2+}, but deactivation kinetics were unaffected (Fig. 8 *B*), even though the membrane potential for both sets of results was approximately the same (−45 and −50 mV, respectively). These results appear to implicate an initial conditioning of the divalent cation effect. Specifically, gating is altered by a change in Ca_o^{2+} when a voltage step is made from a membrane potential negative to rest, whereas gating is unaltered after a depolarizing, conditioning step. This observation requires a rather different mechanism to explain the effects of divalent cations from models previously proposed. A similar "discontinuity" was observed with intracellular divalent cations, although the appearance of the effect was less marked because of the effect of these solutions on the delay preceding activation with a depolarizing step. That is, the tail current time constant after a depolarizing prepulse was increased by 100 Mg_i^{2+} even at $V \sim -50$ mV. Moreover, the time constant of the slow phase of activation at −50 mV from a holding potential of −90 mV was unaltered, as shown for the −20 mV results in Fig. 6 *B*. However, the latter results differed in the delay that preceded activation.

DISCUSSION

The two main observations in this study concern blockade of I_K and modulation of I_K kinetics by divalent cations. Blockade of I_K by Ca_o with a relatively large K_D for the effect has been reported for the *Shaker* K^+ channel (Heginbotham et al., 1992). Surprisingly, this result has not been noted previously for the squid axon delayed rectifier, probably because the blockade is obscured by an effect of Ca_o^{2+} on I_K inactivation (Figs. 3 and 4). The voltage-independence of blockade (Fig. 2) contrasts with the block of I_{Na} by Ca_o^{2+}, which is markedly voltage-dependent. In particular, inward current is blocked, but outward current is relatively unaffected, resulting in a N-shaped current-voltage relation (Yamamoto et al., 1984). The K_D values of block for Mg_o^{2+} and Ca_o^{2+} for the squid I_K channel are quite large, ~500 and 100 mM, respectively. However, the concentrations of these cations in seawater are also relatively large (Mg_o^{2+} = 50 mM; Ca_o^{2+} = 10 mM), which suggests that ~20% of I_K is blocked by these ions under physiological conditions. Moreover, ~25% of I_K is inactivated at rest (Clay, 1989), which suggests that only ~65% of I_K is available for activation during the action potential under physiological conditions.

The primary results in this report relating to modulation of I_K gating concern the effects of intracellular magnesium ions. Specifically, the addition of 100 mM Mg^{2+} to the intracellular perfusate substantially slowed the closing rate of the channel at hyperpolarized potentials with relatively little effect on gating at strongly depolarized potentials, which is the converse of the effects of extracellular divalent cations. The effect of Ca_o^{2+} on gating is about twice as great as that of Mg_o^{2+} under similar conditions, whereas Ca_o^{+} block of I_K is about fivefold more potent than the corresponding effect of Mg_o^{2+}. This result together with the lack of block observed with Mg_i^{2+} suggests that the modulatory and blocking effects of these ions are not directly related. The contrasting effects of intra- and extracellular divalent cations on gating given above compare favorably with similar observations by Cukierman and colleagues concerning the effects of intra- and extracellular divalent cations on gating of the mammalian sodium ion channel (Cukierman et al., 1988; Cukierman and Krueger, 1990, 1991). A further similarity concerns the comparison of effects of Mg_o^{2+} and Mg_i^{2+}, which appear to be about equally potent in shifting the activation curve along the voltage axis. A similar result was reported by Cukierman and Krueger (1991).

The mechanism underlying the effects of divalent cations on gating has not yet been elucidated. The results in Fig. 8 suggest that a novel process may be at work here, such as an initial conditioning of the calcium ion-I_K channel interaction by membrane potential.

REFERENCES

Armstrong, C. M., and G. Cota. 1990. Modification of sodium channel gating by lanthanum. Some effects that cannot be explained by surface charge theory. *J. Gen. Physiol.* 96:1129–1140.

Armstrong, C. M., and D. R. Matteson. 1986. The role of calcium ions in the closing of K channels. *J. Gen. Physiol.* 87:817–832.

Chabala, L. D. 1984. The kinetics of recovery and development of potassium channel inactivation in perfused squid giant axons. *J. Physiol.* 356:193–220.

Clay, J. R. 1985. Comparison of the effects of internal TEA^+ and Cs^+ on potassium current in squid giant axons. *Biophys. J.* 45:481–485.

Clay, J. R. 1989. Slow inactivation and reactivation of the K^+ channel in squid axons. A tail current analysis. *Biophys. J.* 55:407–414.

Clay, J. R. 1990. I_K inactivation in squid axons is shifted along the voltage axis by changes in the intracellular pH. *Biophys. J.* 58:797–801.

Clay, J. R. 1991. A paradox concerning ion permeation of the delayed rectifier potassium ion channel in squid giant axons. *J. Physiol.* 444: 499–511.

Clay, J. R. 1993. Blockade of the delayed rectifier by calcium ions. Relationship to the effects of divalent cations on gating. *Biophys. J.* 64:A312 (Abstr.).

Clay, J. R., and M. F. Shlesinger. 1982. Delayed kinetics of squid axon potassium channels do not always superpose after time translation. *Biophys. J.* 37:677–680.

Clay, J. R., and M. F. Shlesinger. 1983. Effects of external cesium and rubidium on outward potassium currents in squid axons. *Biophys. J.* 42:43–53.

Cole, K. S., and J. W. Moore. 1960. Potassium ion current in the squid giant axon: dynamic characteristic. *Biophys. J.* 1:1–14.

Cukierman, S., and B. K. Krueger. 1990. Modulation of sodium channel gating by external divalent cations studied in planar lipid bilayers. Differential effects on opening and closing rates. *Pfluegers Arch.* 416: 360–369.

Cukierman, S., and B. K. Krueger. 1991. Effects of internal divalent cations on the gating of rat brain Na^+ channels reconstituted in planar lipid bilayers. *Pfluegers Arch.* 419:559–565.

Cukierman, S., W. C. Zinkand, R. F. French, and B. K. Krueger. 1988. Effects of membrane surface charge and calcium on the gating of rat brain sodium channels in planar bilayers. *J. Gen. Physiol.* 92: 431–477.

Ehrenstein, G., and D. L. Gilbert. 1966. Slow changes of potassium permeability in the squid giant axon. *Biophys. J.* 6:553–566.

Frankenhauser, B., and A. L. Hodgkin. 1957. The action of calcium on the electrical properties of squid axons. *J. Physiol.* 137:218–244.

Gilly, W. F., and C. M. Armstrong. 1982a. Slowing of sodium channel opening kinetics in squid axon by extracellular zinc. *J. Gen. Physiol.* 79:935–964.

Gilly, W. F., and C. M. Armstrong. 1982b. Divalent cations and the activation kinetics of potassium channels in squid giant axons. *J. Gen. Physiol.* 79:965–996.

Goldman, D. E. 1943. Potential, impedance, and rectification in membrane. *J. Gen. Physiol.* 27:37–60.

Heginbotham, L., T. Abramson, and R. MacKinnon. 1992. A functional connection between the pores of distantly related ion channels as revealed by mutant K^+ channels. *Science.* 258:1152–1155.

Hodgkin, A. L., and A. F. Huxley. 1952. A quantitative description of membrane current and its application to conduction and excitation in nerve. *J. Physiol.* 117:500–544.

Hodgkin, A. L., and B. Katz. 1949. The effect of sodium ions on the electrical activity of the giant axon of the squid. *J. Physiol.* 108:37–77.

Perozo, E., and F. Bezanilla. 1990. Phosphorylation affects voltage gating of the delayed rectifier K^+ channel by electrostatic interactions. *Neuron.* 5:685- 690.

Spires, S., and T. Begenisich. 1992. Chemical properties of the divalent cation binding site on potassium channels. *J. Gen. Physiol.* 100:181–193.

Yamamoto, D., J. Z. Yeh, and T. Narahashi. 1984. Voltage-dependent calcium block of normal and tetramethrin-modified single sodium channels. *Biophys. J.* 45:337–344.